Journal of Techniques, ISSN: 2708-8383, Vol. 7, No. 4, 2025, Pages 28-36
DOI: https://doi.org/10.51173/jt.v7i4.2653

JOURNAL OF TECHNIQUES

Journal homepage: http://journal.mtu.edu.iq

RESEARCH ARTICLE – ENGINEERING (MISCELLANEOUS)

Vivaldi Antenna Performance Enhancement for IoT Applications Using Optimal Bandwidth

Amina Hashim Issa[1], Mohsen Nickray[1*]

[1]Department of Information Technology Engineering, Faculty of Engineering, University of Qom, Qom, Islamic Republic of Iran

[*] Corresponding author E-mail: m.nickray@qom.ac.ir

Article Info.

Article history:

Received
09 January 2025

Revised
07 August 2025

Accepted
07 October 2025

Published
31 December 2025

Abstract

The dual-band microstrip is designed to be compatible with Internet of Things (IoT) applications, Bluetooth, and Wi-Fi standards, ensuring reliable communication for short- and medium-range IoT devices. Utilizing an FR4 substrate, the antenna achieves excellent return loss, satisfactory gain, and near-omnidirectional radiation patterns, making it ideal for compact IoT devices. This paper presents a dual-band Vivaldi antenna for IoT applications operating at 2.4 GHz and 5.8 GHz. Designed and optimized using ADS software, the antenna achieves a compact layout on FR4 with enhanced return loss and radiation performance. The proposed design achieves a return loss of –32 dB at 2.4 GHz and –17.6 dB at 5.8 GHz, with bandwidths of 660 MHz and 640 MHz, respectively. Radiation efficiencies reached 80% and 78%. These results confirm the antenna's suitability for short- and mid-range wireless protocols such as Wi-Fi and Bluetooth. Future work may explore integration with RF energy harvesting and real-world multipath testing.

Publisher: Middle Technical University

Keywords: Microstrip Vivaldi Antenna; FR4; IOT; Dual Band.

1. Introduction

The expansion of communication technologies on the Internet quickly spread Micro Electromechanical Systems (MEMS), Wireless Sensor Networks (WSN), and the Internet of Things (IoT). Due to its low-profile design, lightweight, and integration into compact devices with operational frequency, the microstrip antenna is highly desirable for IoT applications. For scalability, fault tolerance, energy harvesting, and security-related issues, this would be considered a global acceptance. Additionally, to support integrated services, the antenna system must cover the main frequency bands of IEEE 802.11 and IEEE 802.15.4 while maintaining appropriate gain levels and radiation characteristics [1]. Due to multiple communication standards, IoT devices need antennas that can efficiently operate over different frequency bands. This means that an antenna design, as it is today, has difficulty achieving dual-band or multi-band operation while simultaneously having other high-performance characteristics like low return loss, sufficient gain, and nice radiation properties. The Microstrip antenna Designs mostly have poor features like non-coverage of required frequency bands, lack of proper energy transfer, short communication range, and scope of interference. Therefore, an optimized dual-band Microstrip antenna design for IoT applications is proposed that will work by Bluetooth and Wi-Fi standards, i.e., 802.15.1 and 802.11 ac/ax, respectively. The design covering the entire process includes a detailed simulation for optimizing the parameters of the antenna, and evaluations of the antenna performance are done from parameters like return loss, gain, and radiation patterns in both 2.4 GHz and 5.8 GHz frequency bands [2]. Although many dual-band IoT antennas exist, most either use expensive substrates (e.g., Rogers) or are inefficient when implemented on low-cost FR4. In particular, existing FR4 designs often cover only one band (5.8 GHz) or achieve narrow bandwidths (≤100 MHz at 2.4 GHz), making them ill-suited for compact, battery-powered IoT modules. Existing FR4 designs either cover only one band or achieve narrow bandwidth at 2.4 GHz, making them ill-suited for compact, battery-powered IoT modules. This study proposes a design based on certain assumptions regarding the radiator and ground panels' shapes and dimensions, as well as substrate dimensions, and the FR4 dielectric substrate provides a trade-off between compactness and performance. IoT devices operate in both indoor and outdoor environments, in which wireless communication metrics (return loss and gain) need to be stable. Simulation tools can accurately model the physical behavior of the antenna, and therefore, we can expect that an optimized design will perform similarly in a real-world environment. The dual-band operation at 2.4 GHz and 5.8 GHz can meet the needs of most short - and medium-range communications. This will give a design of a Microstrip antenna fulfilling the specifications of dual-band IoT applications at the frequencies 2.4 GHz and 5.8 GHz. These antenna designs need to be optimized in terms of the dimensions and layout to achieve the lowest return loss and the maximum gain.

Nomenclature & Symbols			
ADS	Advanced Design System (Antenna Simulation Software)	MEMS	Microelectromechanical Systems
dBi	Decibel Isotropic	MIMO	Multiple-Input Multiple-Output
GPS	Global Positioning System	VSWR	Voltage Standing-Wave Ratio
FR4	Flame Retardant	ε_r	Dielectric Constant
IEEE 802.11	Wireless LAN Standard (Wi-Fi)	tan δ	Loss Tangent of the Substrate
IEEE 802.15.4	Wireless Personal Area Network Standard (e.g. Zigbee)	S_{11} (Return Loss)	Input Reflection Coefficient (Scattering Parameter)
IEEE 802.15.1	Bluetooth Standard	UWB	Ultra-Wideband
802.11ac / 802.11ax	High-Speed Wi-Fi Amendments	Wf, Lf	Feed-Line Width (Wf) and Length (Lf)
IoT	Internet of Things	WSN	Wireless Sensor Network

In addition, performance features such as return loss, gain, and radiation patterns will be evaluated by using sophisticated software tools to simulate the antenna. Simulated results can be compared to theoretical standards and benchmarks, to check if the design meets all the specifications requirements for IoT applications. The research presents practical and Effective solution can potentially apply some of the IoT devices are designed to enhance their performance and contribute to the widespread usage of IoT technologies, thereby contributing to IoT technologies. The antenna demonstrates a compact size with an input impedance of 50 Ohms, where return loss was -32.2 dB at 2.4 GHz and -17.6 dB at 5.8 GHz.

The antenna is a critical component in an RF system. It transmits and receives electromagnetic waves, and the high efficiency of an antenna can be transferred to the whole system's efficiency, which will lower the complexity of the receiving process. Some applications require omnidirectional radiation in certain orientations, while other system applications are focused on certain transmissions. It has an antenna design that plays an important role in determining system effectiveness. The rectangular and square patch antennas have high demand due to their low-profile nature [3], making them suitable for aerospace, aircraft, and satellite applications [4]. They are also utilized in governments and commercial arenas. The microstrip antennas are simple and low in cost, employing the modern printed-circuit technology [5, 6]. Using loads, a significant reconfiguration of resonant frequency, polarization, radiation pattern, and impedance can be achieved. Essentially, a microstrip antenna comprises a metallic patch placed on top of a ground plane with a dielectric substrate in between. The general types are rectangular and circular patches. Due to their low profile, light weight, and ease of integration, Microstrip antennas are highly suitable for use in modern compact devices, such as those utilized in IoT networks [4, 7]. The Vivaldi antenna is a planar, broadband antenna characterized by its tapered slot configuration. This unique geometry enables it to operate effectively across a wide range of frequencies, making it a versatile choice for numerous wireless applications. Moreover, the simplicity of design and ease of fabrication contribute to its popularity [8]. An antenna array consists of multiple antennas, arranged geometrically, to achieve specific patterns of the antenna, such as increased gain, better polarization, and reduced secondary lobes. The intelligent combination of basic radiation elements can emit a variety of unique radiation patterns. The electromagnetic fields from an antenna array are vectorially added to create radiation. Linear, circular, planar, or non-planar, the array can also have asymmetrical distribution. To facilitate 3D scanning while maintaining low levels of side lobes, planar arrays can be used instead of linear arrays with their fan-shaped radiation pattern [9-12]. As previously mentioned, the properties of antennas such as directivity, gain, reflection coefficient, radiation pattern, and polarization greatly affect their performance. Directivity is the ratio of the intensity of radiation in a given direction to the average intensity of radiation in all directions, and it describes how efficiently energy is concentrated in a given direction. Gain, in contrast, is the ratio of the intensity in a given direction to that which would be received if the antenna radiated power isotropically. It also indicates the directionality and strength of the antenna and helps assess how well an antenna directs energy [13]. The reflection coefficient indicates the quality of the match between the antenna and the input transmission line. With an appropriately matched antenna, there will be no reflected signals, and a significant portion of the RF power will be transmitted into the free space. Reducing the reflection coefficient is essential to improving the efficiency of the antenna and the performance of the overall system. For an antenna to be considered well-matched, 10% or less of the signal must be reflected, or equivalently, the reflection coefficient must be −10 or better, as radiation patterns are defined. The radiation pattern is defined as the geometric arrangement of the radiated energy for the far-field region. The two basic radiation patterns are used: the field pattern (electric field) and the power pattern (magnetic field). There are different types, where the uniform radiation is preferred in mobile communication, which are omnidirectional antennas, whereas a directional antenna is favored in radar applications due to focused radiation [14].

2. Literature review

In Gocen et al., a microstrip patch antenna for IoT applications at the 5.8 GHz band was designed [15]. A full circle, a semicircle, and a meander line are all small parts of the overall size of the proposed antenna. This article covers antenna performance, and the results indicate that by modifying the dimensions of the square ground plane, antenna gain and efficiency can be increased. The return loss of 700 MHz bandwidth in the 5.8 GHz band for the proposed antenna was less than -20 dB with 4.35 dBi. – 8.5 GHz frequency bands under various bands of the 4.5 GHz [15] multi-band system [14]. Soundharya et al. launched a UWB GPS antenna for military communications, satellite systems, and cognitive radio systems. The subtracted material in the antenna is rectangular, which is simply known as FR4, and Microstrip feeding is used for the same. This is either a little 20 x 15 mm² antenna with a 1.6 mm thick geometry , single patch type, and so enables optimization to keep the UWB spec standard. Return loss (S11) performance versus frequency indicates stable and consistent bandwidth across the entire operating range of the antenna. A W-slot can be defected on the radiating patch to improve UWB performance [16]. Huange et al. Designed a quad-port MIMO antenna array for a 5G smartphone application. The array is made up of four elements deployed on two sideboards with dimensions of 14.9 mm x 7 mm x 0.8 mm. It was introduced, considering the following in this configuration, dividing the antenna into four parts: the L-shaped feeding, the rectangular parasitic strip, the strip and Z-shaped radiation strip, a parametric analysis of the antenna is performed, optimized for a system working in both bands at 3.5 GHz and 5 GHz, with an efficiency of 82%, isolation of 16.5 dB and gains in total of 4.7 dBi and 5 dBi, respectively [17]. Hussain et al. (2019) proposed a compact meandered loop slot-line antenna for 5G Internet of Things (IoT) applications. The design enables long-range communication while maintaining low power consumption, making it well-suited for operation in the sub-GHz frequency band. The antenna, which incorporates a meandered loop slot-line loaded with a varactor diode, offers wideband frequency tunability.

It operates within a frequency range of 758–1034 MHz, with a minimum bandwidth of 17 MHz. The antenna is fabricated on an RO4350 substrate and achieves an efficiency of 54–67% and a gain ranging from 0.86 to 1.8 dBi [18].

Faouri et al. proposed a compact Microstrip meandered bowtie antenna with multiple resonant frequencies and several rejection bands, which can be used in 5G applications. For a double-sided FR-4 substrate, the gain achieved by using this dual-band high-efficiency antenna (90.3%) is 4.46 dB. It operates the S, C, and X bands (i.e., at the resonant frequencies located at 2.7, 4.05, 5.05, 6.04, 7.15, 7.9, and 11.55 GHz [19]). Baccouch et al. 5G mobile communication based on a hybrid antenna design and solar cells [20]. The antenna is equipped with a mesh patch on the front surface, combining solar energy harvesting with RF communication. Those will be the new frequency bands for 5G standard, 2.6 GHz, and 3.5 GHz. The performance results were quite promising with a reflection coefficient of −23.82 dB at 2.6 GHz and −39.96 dB at 3.5 GHz [21]. Marzouk et al. proposed three low-profile Microstrip line-fed planar MIMO antennas for 5G mobile communication. Design 1 is a two-element rectangular patch antenna. In contrast, Design 2 is a symmetric dual-band antenna containing slotted rectangular patches, and Design 3 proposes a symmetric dual-band four-element antenna with slotted rectangular patches. The antennas offer enhanced return loss and wideband, and low mutual coupling without additional structures. The antennas have good directivity, gain, and radiation efficiency, and can be used in 5G applications. The antennas were manufactured using a photolithography process and characterized with a Vector Network Analyzer ZVA 67 [22]. Khan et al. [20] proposed a compact ultra-wideband antenna measuring 24 × 28 mm, which supports Bluetooth version 5 and is compatible with ultra-wideband communication up to 440 kb/s. It also supports MIFARE cards and ISO 14443 Type A/B standards, facilitating integration into mobile devices. The antenna design ensures low power return loss and reduced mutual coupling, making it suitable for MIMO applications. Three cylindrical surface configurations are described: independent, clustered, and conformal arrays. The initial single-element antenna was further developed into an array to achieve higher gain and improved axial directional performance. The complete antenna system operates in the 9 GHz band, as reported in [23].

3. Methodology and Methods

Compact patch antennas have been designed for Internet of Things (IoT) devices. The design was carried out on FR4 substrate due to its suitable dielectric properties and economic feasibility. The design was simulated and realized on the Advanced Design System (ADS) software to view vital performance parameters like return loss, surface current distribution, radiation patterns, gain, and directivity for frequencies ranging from 0 GHz up to 10 GHz.

FR4 ($\varepsilon_r = 4.4$, $\tan\delta = 0.02$, thickness = 0.8 mm) is selected for its low cost and ease of fabrication. The radiator started as a rectangular patch: a vertical slot was introduced to tune the 2.4 GHz resonance, and two lateral slots excited a 5.8 GHz mode without increasing footprint. A ground-plane cutout was added to shift current paths and widen bandwidth at both bands.

3.1. Substrate

The design process for a Microstrip patch antenna involves selecting the substrate material and determining its thickness. The choice of dielectric material and its thickness is crucial for optimizing antenna performance. The suggested antenna is designed on an FR4 dielectric substrate with a dielectric constant of εr=4.4 and a thickness of 0.8 mm, and a loss tangent of 0.02. Fig. 1 indicates the substrate selected, and Fig. 2 describes the substrate dimensions of this substrate.

3.2. Radiator

The radiator is based on a rectangular shape with a main patch of width 17.400 mm and a total length of 21.3 mm. The top region has a width of 13.400 mm with a height of 0.7 mm. There is a longer vertical slot, L3, placed centrally in the main patch region; two other slots, L4 and L2, are placed on the edges, and a triangular region of width 5.7 mm. The feed line has a width (Wf) of 2.0 mm, which starts from the bottom of the patch and has a length (Lf) of 15.3 mm to give enough attached area to the external circuitry. The feeding line is symmetrically placed at the center for good current distribution and impedance matching for effective antenna operation. The proposed antenna features a unique rectangular radiator with three strategically placed slots and a triangular top region. This geometry optimizes current distribution, enabling dual-band resonance with minimal return loss. Fig. 3 shows the dimensions of the radiator.

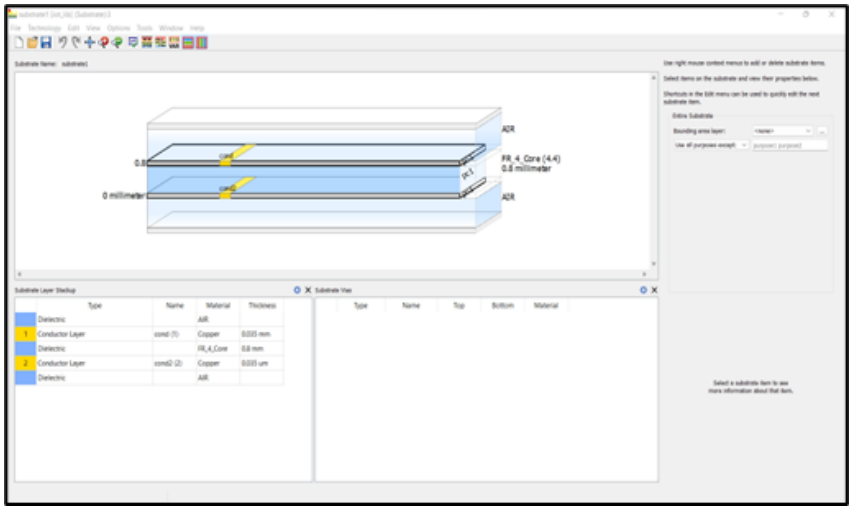

Fig. 1. The selected substrate

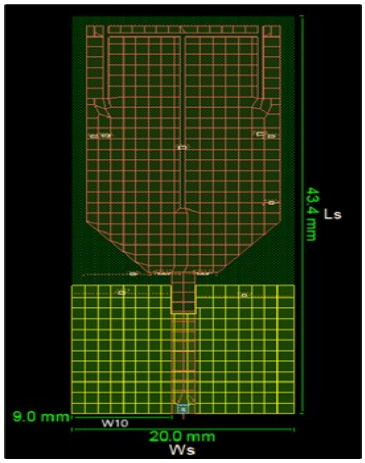

Fig. 2. Substrate dimensions

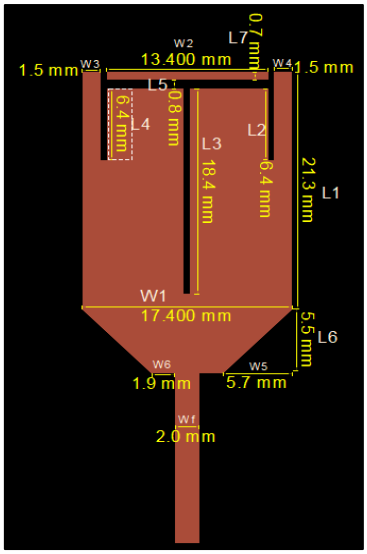

Fig. 3. Radiator dimensions

3.3. Ground plane

The design of the ground plane is a rectangular structure having a cutout in the upper portion of its length. The total length of the ground plane is 14.0 mm, and the total width is 20.0 mm. The dimensions of the proposed antenna have been hand-tuned to get the best performance in impedance matching and return loss to obtain a proper signal transmission and reception within the desired frequency of operation. Fig. 4 shows the dimensions of the ground plane. This work introduces a ground plane cutout and multi-slot radiator to achieve superior return loss in a compact, low-cost form factor, addressing key IoT constraints overlooked in prior art.

Fig. 4. Ground plane dimensions

3.4. The final design

In conclusion, the proposed antenna is optimized to be compatible with Bluetooth and Wi-Fi standards in order to be reliable over most common IoT communication bands, especially at 2.4 GHz and 5.8 GHz. Fig. 5 represents the final 3D design of the antenna. Table 1 summarizes the key dimensions of the proposed antenna, which include the patch, the ground plane, and other critical design elements as defined in the previous sections. Table 2 represents a concise reference guide that defines the key technical terms, symbols, and parameters used throughout the paper.

Table 1. Dimensions of the proposed antenna (mm)

Dimension	Value	Dimension	Value
L1	21.3	W1	17.4
L2	6.4	W 2	13.4
L3	18.4	W 3	1.5
L4	6.4	W 4	1.5
L5	0.8	W 5	5.7
L6	5.5	W 6	1.9
L7	0.7	W 7	2.2
L8	3.1	W 8	8.9
L9	14.0	W 9	8.9
Lf	5.3	W10	9.0
Ls	43.4	Wf	2.2
-	-	Ws	20.0

Table 2. Define the key technical terms

Symbol	Definition
Bi	Decibels relative to an isotropic radiator. An isotropic radiator is a theoretical point source that emits or receives equally in all directions.
S_{11} (Return Loss)	Input reflection coefficient at the antenna port, expressed in dB. Indicates how much power is reflected toward the source.
VSWR	Voltage Standing-Wave Ratio. Ratio of maximum to minimum voltage on the feed line.
ε_r	Relative permittivity (dielectric constant) of the substrate material, dimensionless.
tan δ	Loss tangent of the substrate. Represents dielectric losses, dimensionless.
Wf, Lf	Feed-line width and length (mm). Determines impedance matching and physical connection to external circuitry.
FR4	Epoxy-glass laminate substrate (ε_r=4.4, tan δ≈0.02) is commonly used in PCB and antenna fabrication.

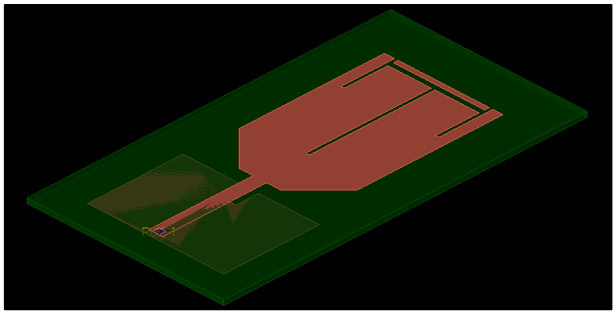

Fig. 5. Final 3D design of the antenna

4. Results and Analysis

This section considers the performance of the proposed antenna at 2.4 GHz and 5.8 GHz, which are Wi-Fi and Bluetooth protocols, respectively. The result is indicative of how this antenna will perform well in these respective frequency bands. The antenna was designed and simulated on ADS software, sweeping from 0 GHz to 10 GHz, with an increment of 0.02 GHz. Different simulations were carried out in order to analyze important parameters of the antenna performance, which included return loss, surface current distribution, radiation pattern, directivity, and gain. Characteristics were analyzed in order to check the efficiency and efficacy of the antenna within the putative frequency ranges, specifically at 2.4 GHz and 5.8 GHz, which are imperative for IoT applications.

4.1. Results at 2.4 GHz

In this section, the simulation results at 2.4 GHz are presented.

4.1.1. Return loss

The antenna's lower band covers the frequency range from 2.18 GHz to 2.84 GHz, providing a bandwidth of 0.66 GHz. It demonstrates strong performance at 2.4 GHz, with a return loss of -32 dB, making it well-suited for IoT applications. Fig. 6. Simulated return loss (S_{11}) vs. frequency of the proposed Antenna. Indicate that the antenna's lower band covers the frequency range from 2.18 GHz to 2.84 GHz, providing a bandwidth of 0.66 GHz. Within this range, the antenna demonstrates strong performance at 2.4 GHz, with a return loss of -32 dB. This significant return loss indicates excellent impedance matching at this frequency, making the antenna well-suited for IoT applications operating in the 2.4 GHz band.

Microstrip feed-line position: The feed line is centered under the patch. Moving it laterally by ±0.5 mm shifts the 2.4 GHz matching point by up to 100 MHz. Central placement ensured symmetric excitation and a smooth S_{11} curve.

Microstrip feed-line length (Lf = 15.3 mm): Lf acts as a quarter-wave transformer at 2.4 GHz. Increasing Lf by 1 mm improved the return loss at 2.4 GHz by 3 dB but narrowed the bandwidth. Lf = 15.3 mm provided the best trade-off: deep match and 660 MHz bandwidth. Central slot length (L3 = 18.4 mm): L3 sets the half-wave resonance at 2.4 GHz. Shortening L3 shifts the resonance upward and reduces the lower-band bandwidth. L3 = 18.4 mm aligns the 2.4 GHz resonance and maximizes its 660 MHz span.

Slot widths (W3, W4 = 1.5 mm): Slot width controls capacitive coupling between patch and ground plane. W3, W4 = 1.5 mm flattened the S_{11} response at both bands. Narrower slots (< 1.2 mm) deepened the notch but shrank bandwidth; wider slots (> 1.8 mm) raised S_{11}.

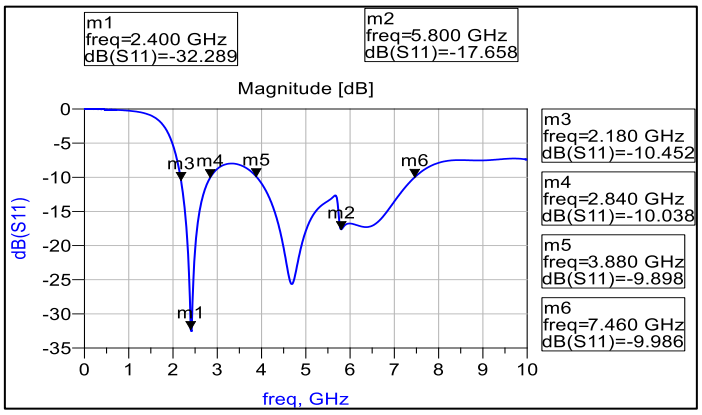

Fig. 6. The proposed Antenna's return loss

4.1.2. Surface current distribution at 2.4 GHz

Fig. 7 shows that the surface current distribution of the antenna is concentrated along the narrow edges of the feed line, the upper edges of the ground plane, and the lower edges of the radiator, contributing to efficient operation. The current is predominantly concentrated along the edges of the narrow feed line, the upper edges of the ground plane, and the lower edges of the radiator. This current flow pattern suggests that these regions play a critical role in the antenna's radiation characteristics and performance at this frequency, contributing to efficient operation in the 2.4 GHz band.

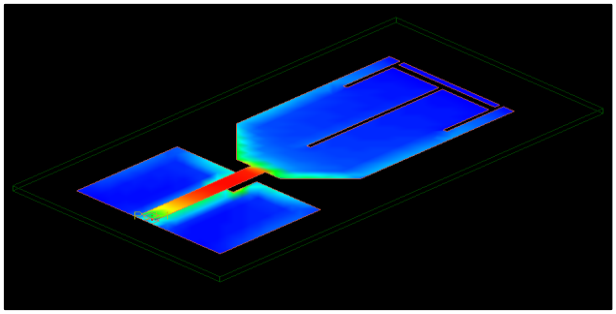

Fig. 7. Surface current distribution at 2.4 GHz

4.1.3. Radiation pattern

The radiation pattern shows near-omnidirectional radiation, ensuring consistent signal coverage and reliable communication regardless of the antenna's orientation. Fig. 8 demonstrates that the antenna exhibits near-omnidirectional radiation, with energy being radiated almost equally in all directions. This characteristic is advantageous for IoT applications, as it ensures consistent signal coverage and reliable communication regardless of the antenna's orientation. Such radiation behavior enhances the antenna's suitability for environments where uniform coverage is critical.

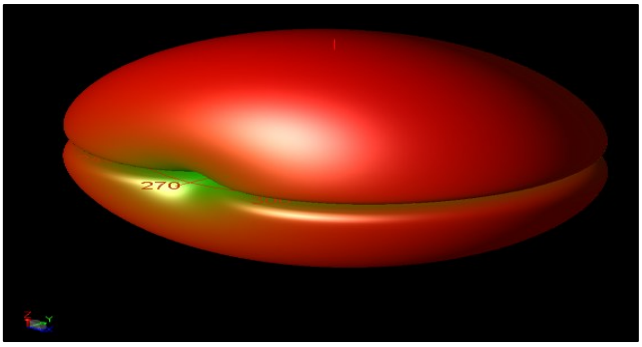

Fig. 8. 3D radiation pattern at 2.4 GHz

4.1.4. Directivity and gain

The antenna achieves a directivity of 2.5 dBi and a gain of 1.6 dBi, indicating moderate directionality and efficiency in transmitting power. The radiation efficiency is recorded at 80%, indicating that a large fraction of the input power is indeed radiated in the form of electromagnetic waves. The radiation pattern is near-omnidirectional in the H-plane, making it ideal for short-range indoor IoT coverage (e.g., Wi-Fi, BLE). The E-plane shows a symmetrical main lobe with moderate elevation gain. Fig. 9 shows the directivity and gain of the proposed Antenna at 2.4

GHz. These values indicate that while the antenna radiates almost equally in all directions, it still provides a moderate level of directionality and efficiency in transmitting power. The combination of this directivity and gain further confirms the antenna's effectiveness for short- to medium-range IoT applications, where consistent performance and reliable communication are essential.

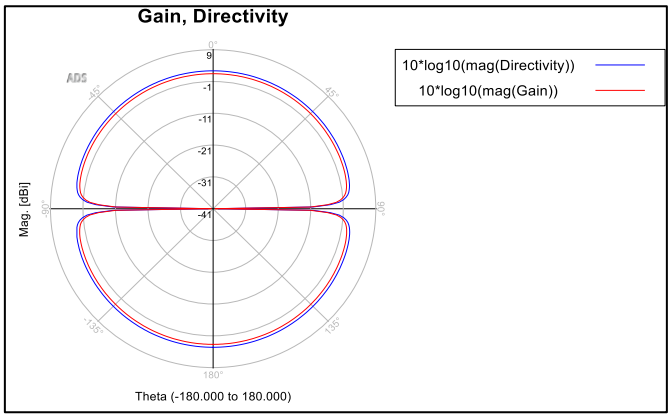

Fig. 9. Directivity and gain at 2.4 GHz

4.2. Results at 5.8 GHz

In this section, the results of the simulations at 5.8 GHz are shown.

4.2.1. Return loss

Fig. 6 shows the results of the simulation. The results show that the antenna's upper band operates efficiently at 5.8 GHz, with a return loss of -17.6 dB, indicating good impedance matching.

4.2.2. Surface current distribution at 5.8 GHz

The 5.8 GHz surface current distribution is primarily along the edges of the narrow feed line and the highest edges of the radiator, particularly around strip-shaped openings, as shown in Fig. 10. This distribution highlights the critical regions of the antenna that contribute to its performance at 5.8 GHz, influencing the radiation characteristics and ensuring efficient operation within this frequency band.

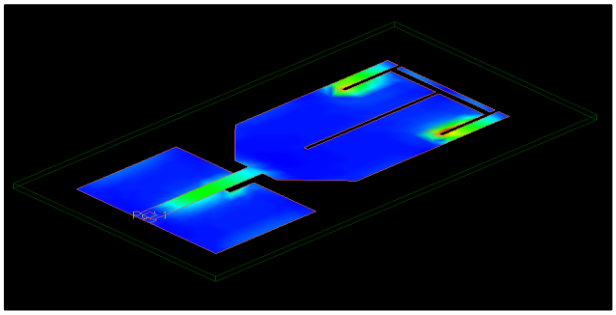

Fig. 10. Surface current distribution at 5.8 GHz

4.2.3. Radiation pattern

The 5.8 GHz radiation pattern is near omnidirectional with good energy distribution around the antenna, which supports efficient signal reception and transmission over a wide range of angles. Fig. 11 shows the 3D radiation pattern at the 5.8 GHz frequency. The energy is distributed somewhat evenly around the antenna; this pattern also supports efficient signal reception and transmission across a wide range of angles, which is important for maintaining reliable communication in diverse IoT environments.

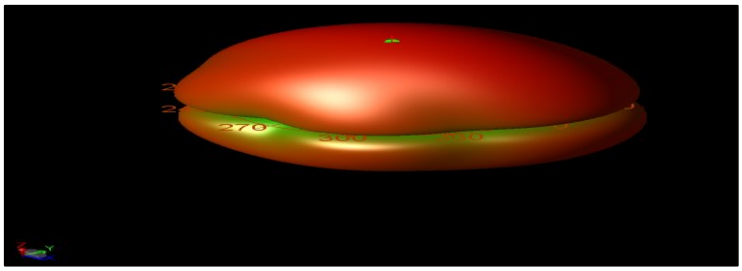

Fig. 11. 3D radiation pattern at 5.8 GHz

4.2.4. Directivity and gain

The antenna's directivity and gain are also measured, and the directivity is 4.25 dBi. In comparison, the gain is 2.29 dBi, showing the overall efficiency of the antenna in converting input power into radiated energy. Fig. 12 shows the proposed Antenna's directivity and gain at 5.8 GHz.

The antenna radiates in all directions with varying intensity levels. The directivity at 5.8 GHz is measured to be 4.25 dBi, indicating a stronger focus of radiated energy in certain directions. Additionally, the gain is observed to be 2.29 dBi, which reflects the overall efficiency of the antenna in converting input power into radiated energy.

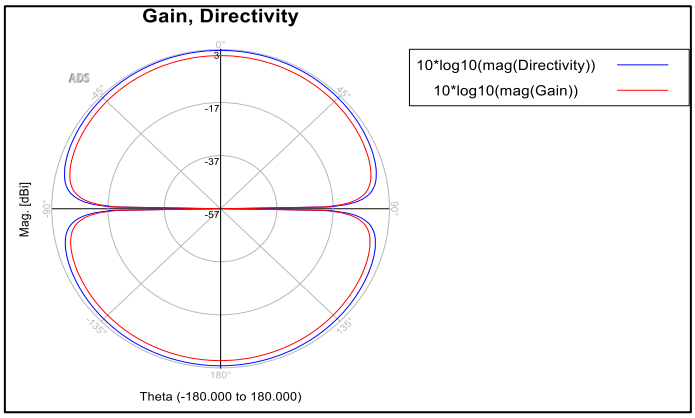

Fig. 12. Antenna gain and directivity at 5.8 GHz

4.3. Discussion

The design and simulation of this work is to be used for an Antenna suitable as a Microstrip for IoT applications at 2.4 GHz and 5.8 GHz. The return loss and bandwidth analysis provide us with the return loss of -32 dB at 2.4 GHz showing one band while the second operating band shows return loss of -17.6 dB at 5.8 GHz. In the case of 2.4 GHZ, the surface current distribution is along the surface of the patch-shaped radiators, suggesting an omnidirectional pattern, while at 5.8 GHZ, the surface currents are focused on the smaller feed line as well as adjacent to the strip-shaped corners in the radiator. At 2.4 GHz, the radiation pattern is almost omnidirectional (D = 2.5 dBi, G = 1.6 dBi) while at 5.8 GHz it is more directive (D = 4.25 dBi, G = 2.29 dBi). The antenna performance is also shown in both frequency bands, so the presented antenna can be utilized in most IoT applications. The accurate impedance matching, typical gain, and directivity characteristics ensure consistent and reliable communication in a fluctuating IoT environment. And its use of frequencies is versatile enough that it is a very valid choice for both consumer electronics and industrial IoT networks. In typical IoT nodes, a return loss of –10 dB or better ensures minimal power wasted on reflections. Our antenna's S_{11} of –32 dB at 2.4 GHz (≈0.25 % reflection) and –17.6 dB at 5.8 GHz (≈1.7 % reflection) far exceed this, reducing retransmissions and saving battery life. With 1.6 dBi gain and 80 % efficiency at 2.4 GHz, and 2.29 dBi gain with 75 % efficiency at 5.8 GHz, it supports reliable 10 m indoor links while allowing lower transmit power. The 43.4 × 20 mm (≈900 mm²) footprint also leaves ample PCB space for sensors, controllers, and batteries, meeting compactness needs. The simulation results demonstrate that the designed microstrip antenna performs effectively in both the 2.4 GHz and 5.8 GHz frequency bands, making it suitable for a wide range of IoT applications. The antenna's excellent impedance matching, combined with favorable gain and directivity characteristics, ensures stable and efficient communication in diverse IoT environments. Its adaptability across different frequencies allows for its use in various IoT devices, from low-power sensors to systems requiring higher data rates. This makes the antenna a strong candidate for both consumer electronics and industrial IoT networks.

4.4. Comparison with existing works

To demonstrate the relative performance and efficiency of the proposed dual-band antenna (operating at 2.4 GHz and 5.8 GHz), Table 3 summarizes key figures of merit from several recent designs reported in the literature. In each case, we compare substrate, operating frequencies, Return Loss, and radiation efficiency. Where appropriate, also note whether a design is single-band or multi-band.

Table 3. Comparison of Recent Dual-Band IoT Antennas

Design & Year	Substrate	Size mm²	Bands (GHz)	Return Loss (dB)	Eff. (%)	Notes
Gocen et al. (2022) [15]	FR4 (ε_r=4.4, tan δ=0.02)	15 × 40	5.8 (single-band)	–20.0	80.6	Single-band only; does not support 2.4 GHz
Faouri et al. (2022) [19]	FR4 (ε_r=4.4)	30 × 30	2.7 / 4.05 / 5.05–11.55 (multi-band)	-18.0 to –25.0	90.3	Multi-band; not optimized for 2.4 GHz
Hussain et al. (2022) [18]	RO4350 (ε_r=3.48)	27 × 60	0.758–1.034 (tunable)	–17.0 to 28.0	54–67	Sub-GHz slot-loop; not relevant to 2.4/5.8 GHz
Jusoh et al. (2023) [24]	FR-4 (ε_r=4.3, 1.6 mm)	20 × 24.8	2.448 / 2.864 / 5.8	–13.872 / –33.491 / –19.3	-	Ring-monopole; 57.8 % miniaturization; measurements validate simulations.
Proposed (2025)	FR4 (ε_r=4.4)	43.4 × 20	2.4 / 5.8	–32.0 / –17.6	80/78	Compact dual-band FR4 design; optimized for IoT (Wi-Fi/Bluetooth)

The proposed antenna achieves its deepest impedance match at 2.4 GHz (–32.0 dB), surpassing every listed design and minimizing power loss. It delivers true dual-band coverage, unlike Gocen's single-band design and Faouri's non-optimized multi-band solution. According to Jusoh et al. (2023), their RCSRR-loaded ring-monopole antenna on a 496 mm² footprint only reached –13.872 dB at 2.448 GHz; our antenna more than doubles that matching depth while still reducing its footprint to 868 mm² and achieving ≥ 78 % efficiency. Unlike Hussain's sub-GHz design, it supports standard Wi-Fi and Bluetooth bands. Overall, our design balances compactness (43.4 × 20 mm, 12 % smaller than Faouri et al.'s 900 mm²), efficiency, and dual-band performance more effectively than all compared antennas.

5. Conclusion

Recently, a dual-band microstrip antenna has been designed and demonstrated for IoT applications that operate at RF frequencies of 2.4 GHz and 5.8 GHz. The antenna shows a very good performance, in terms of weak return loss and good gain of the antenna, making it a potential candidate for various IoT applications. This will be a great starting point to promote antenna development in IoT networks. Future works may include the extension of frequency bands for more emerging IoT applications, as well as the inclusion of energy harvesting modules to improve the antenna's performance in self-powered IoT devices. In addition, future designs may incorporate rectifier circuits or power management units to enable RF energy harvesting, particularly for low-power IoT nodes. These developments would complement the antenna in the new standards for IoT networks of the future.

Acknowledgment

The authors gratefully acknowledge the support of the Department of Electronic Technologies at the Faculty of Engineering at the University of Qom. Special thanks to the technical staff for access to the ADS simulation facilities.

References

[1] W-S. Kim and J-H. Yoon, "A design for a CPW-fed monopole antenna with two modified half circular rings for WLAN/WiMAX operations," J. Inf. Commun. Converg. Eng., vol. 13, no. 3, pp. 159–166, 2015.
[2] Elfergani et al., "Miniaturized balanced antenna with integrated balun for practical LTE applications," Radioengineering, vol. 26, no. 2, pp. 444–452, 2017.
[3] C. A. Balanis, "Horn antennas," in Antenna Handbook, R. C. Johnson, Ed., Springer, 1988, pp. 431–516.
[4] R. M. H. O. I. J., "An overview of the microstrip antenna," ResearchGate, 2016. (Source type unclear).
[5] J. Q. Howell, "Microstrip antennas," Proc. IEEE, vol. 63, no. 1, pp. 90–100, 1975.
[6] D. M. Pozar, "Microstrip antennas," Proc. IEEE, vol. 80, no. 1, pp. 79–91, 1992.
[7] W. F. Richards, "Microstrip antennas," in Antenna Handbook, R. C. Johnson, Ed., Springer, 1988, pp. 639–712.
[8] P. Di Barba and L. Januszkiewicz, "Optimal design of Vivaldi antenna with corner reflector using a multiobjective minimax method," Arch. Electr. Eng., vol. 73, no. 4, pp. 1161–1181, 2024.
[9] C. A. Balanis, Antenna Theory: Analysis and Design, 4th ed., Wiley, 2016.
[10] A. Alzubedy, S. K. Gharghan, M. A. Eldosoky, and A. M. Soliman, "Wireless Power Transfer for Biomedical Implants using Series–Parallel Spider-Web Coil Configuration", EETJ, vol. 2, no. 2, pp. 33–38, Jun. 2025.
[11] J. Lin et al., "A filtering microstrip antenna array," IEEE Trans. Microw. Theory Techn., vol. 59, no. 2, pp. 542–550, 2011.
[12] H. A. Khalaf, "Smart Homes Network Security Issues and Solutions IOT", IJDS, vol. 3, no. 1, pp. 29–44, Nov. 2025.
[13] A.S. Debele, "Review of multiband antenna for mobile communication," J. Electr. Eng. Electron. Control Comput. Sci., vol. 7, no. 1, pp. 43–50, 2020.
[14] S. Elaluf-Calderwood, B. Eaton, and J. Herzhoff, "Mobile platforms as convergent systems—analyzing control points and tussles," in LSE Research Online, pp. 97–112, 2012.
[15] C. Gocen, S. Dulluc, and I. Akdag, "5.8 GHz band Wi-Fi and IoT applications antenna design," ICONTECH Int. J., vol. 6, no. 1, pp. 42–47, 2022.
[16] D. Soundharya, N. Thitha, and L. Priyadharshini, "Design of ultra-wide band antenna," Int. J. Electron. Commun. Eng., vol. 5, no. 6, pp. 7–10, 2019.
[17] J. Huang et al., "A quad-port dual-band MIMO antenna array for 5G smartphone applications," Electronics, vol. 10, no. 5, p. 542, 2021.
[18] R. Hussain et al., "A compact sub-GHz wide tunable antenna design for IoT applications," Electronics, vol. 11, no. 7, p. 1074, 2022.
[19] Y. S. Faouri et al., "A novel meander bowtie-shaped antenna with multi-resonant and rejection bands for modern 5G communications," Electronics, vol. 11, no. 5, p. 821, 2022.
[20] H. M. Newman, "BACnet today and the smart grid," BACnet Int., 2013.
[21] H. Marzouk, M. I. Ahmed, and A. H. A. Shaalan, "Novel dual-band 28/38 GHz MIMO antennas for 5G mobile applications," Prog. Electromagn. Res. C, vol. 93, pp. 103–117, 2019.
[22] M. A. Khan, M. A. Ul Haq, and S. Ur Rehman, "A practical miniature antenna design for future IoT-enabled smart devices," in Proc. ICSPCS, 10th Int. Conf. on Signal Processing and Communication Systems, 2016.
[23] A. Jusoh et al., "Design of miniaturized antenna for IoT using metamaterial," IIUM Eng. J., vol. 24, no. 1, pp. 122–137, 2023.
[24] J. Nafack Nihako et al., "Realistic modeling of photovoltaic solar cell: A simple and accurate two-diode model," IEEE Access, vol. 4, no. 2, pp. 396–400, 2025.